

---

## Vision-based neuro-fuzzy control of weld penetration in gas tungsten arc welding of thin sheets

---

Chuan Song Wu\* and J.Q. Gao

Institute of Materials Joining,  
Shandong University,  
Jinan 250061, China

E-mail: wucs@sdu.edu.cn E-mail: jqg@sdu.edu.cn

\*Corresponding author

**Abstract:** This paper develops a vision-based neuro-fuzzy system to control the weld joint penetration in Gas Tungsten Arc Welding (GTAW) of thin sheets. To this end, a camera equipped with a specially designed composite light-filter is used to observe the weld pool from the topside of the workpiece so that comparatively distinct images of the weld pool are obtained. As the Backside weld Width (BW) reflects the degree of the weld joint penetration, a model describing the relationship between the weld pool surface geometrical parameters (which can be extracted from the weld pool images) and the backside weld width is constructed. A neuro-fuzzy controller and a learning algorithm are developed to address dynamic and non-linear characteristics of the welding process. The controller can learn fuzzy rules and adjust the fuzzy rules with the variation of welding conditions automatically. Simulation and control tests demonstrated the effectiveness of the developed control system.

**Keywords:** neuro-fuzzy control; vision sensor; modelling; weld penetration; Gas Tungsten Arc Welding (GTAW).

**Reference** to this paper should be made as follows: Wu, C.S. and Gao, J.Q. (2006) 'Vision-based neuro-fuzzy control of weld penetration in gas tungsten arc welding of thin sheets', *Int. J. Modelling, Identification and Control*, Vol. 1, No. 2, pp.126–132.

**Biographical notes:** Chuan Song Wu is a Professor and the Director of the Institute for Materials Joining at Shandong University in China. He received his BS, MS and PhD from Harbin Institute of Technology, Harbin, China, in 1982, 1984 and 1988, respectively. He made research stay at the University of Wisconsin-Milwaukee in the USA (Visiting Scholar, 1986–1987), Technical University of Berlin in Germany (Humboldt Scholar, 1993–1995) and Osaka University in Japan (Guest Professor, 1995–1996). Since 2002, he has visited the University of Kentucky in the USA three times for joint research. His current research deals with modelling, sensing and control of welding processes. He has authored and coauthored more than 120 technical papers and two books. He is a member of the standing council of the Chinese Welding Society, the Chairman of Computer-Aided Welding Commission of Chinese Welding Society and a member of the American Welding Society.

J.Q. Gao is an Associate Professor in the Institute for Materials Joining at Shandong University in China. He received a Bachelor's degree in 1993 from the Shandong Institute of Technology, a Master's degree in 1996 from the Harbin Institute of Technology and a PhD in 2000 from Shandong University. In 2005, he made a three-month research stay at the Technical University of Berlin in Germany. His research interests include vision-based sensing and control of arc welding and simulation of welding residual stresses. He has authored and coauthored more than 20 technical papers. He is a member of the Computer-Aided Welding Commission of the Chinese Welding Society.

---

### 1 Introduction

The Gas Tungsten Arc Welding (GTAW) process is widely used for joining of thin sheets in industry. As there are many disturbances in the welding process (such as heat dissipation, small variations in the shape of the part and part fixturing, subtle change in the material composition, variations in the joint fit-up, electrode shape and electrode standoff and thermal distortion of workpiece), automatic control, especially weld penetration

control is needed to assure the weld quality (Pietrzak and Packer, 1994). To this end, sufficient information about weld penetration must be obtained. Unfortunately, it has been a difficult task to directly obtain this information.

Weld pool images can provide abundant weld penetration information (Kovacevic et al., 1996). They can be captured from the topside of the workpiece by a visual sensor. The Backside weld Width (BW), which measures the weld penetration can be predicted from the topside surface geometrical parameters of the weld pool.

Therefore, it is of great significance to develop a system for controlling the weld penetration through sensing the topside geometrical parameters of the weld pool, correlating them to the BW and predicting the degree of penetration based on the BW.

Owing to the high non-linearity, strong coupling among the welding parameters and time-dependence of the welding process, satisfactory results are difficult to obtain by employing conventional control methods (Gao and Wu, 2001; Kovacevic and Zhang, 1995). Thus, it is important to design a robust controller to control weld penetration. Fuzzy control that emulates human behaviour in uncertain environment using fuzzy rules does not require exact mathematical model of the welding system that appears promising. It is especially suitable for complicated systems. However, there are a few weaknesses in obtaining rules from the experience or performance and revising control strategy automatically. Neural network has the characteristics of self-learning and self-organisation for information processing. It also has good self-learning ability to directly obtain knowledge from the experience or performance. However, its convergence is slow and its physical meaning is not clear. Therefore, the methods that combine the neural network with fuzzy control are put forward. Generally, fuzzy system can be used as pre- and postprocessor to a neural network model (Huang et al., 1996; Zhang, 1997).

In this study, the weld pool image is captured from the topside of the workpiece employing a commercial CCD camera with aid of narrow-band pass filter, then surface geometrical parameters of the weld pool is extracted by image processing algorithm, and a model describing the relationship between the surface geometrical parameters of the weld pool and the BW is developed. Such a model is called a FBW (*Front* geometrical parameters of weld pool and *Backside* weld *Width*) model. With this model, the BW is predicted online. Also a neuro-fuzzy controller is designed to realise the weld penetration control.

## 2 Experimental system

A block diagram of the experimental system is shown in Figure 1. The major functional elements of the experimental system include a host computer, a welding control unit, an image capturing board, a CCD camera with narrow-band composite light-filter, a GTAW power supply, a worktable, a welding speed controller and a monitor. Information on the weld pool image captured by the CCD camera with narrow-band composite light-filter is sent to a host computer via the image capturing board (frame-grabber), and then processed to get geometrical parameters of the weld pool. On the basis of these parameters and the model established in this study, a strategy is made to control the welding power supply and the welding speed controller via the welding control unit, thus achieving automatic control of weld penetration.

Once the image of the weld pool captured by the vision sensor is digitised through frame-grabber, it is stored in a computer as a matrix in which one element represents

a dot of the image. A brighter dot in the image corresponds to a higher value (grey value) of the element in the matrix. Coordinates of a point of the image are expressed by  $(i, j)$ . The grey value of point  $(i, j)$  is written as  $g_0(i, j)$ . In the captured images, the pool surface is mirror-like reflection while the solid surface of the workpiece diffusely reflects arc light, so there is a bright region inside the weld pool (Figure 2).

**Figure 1** The block diagram of the system

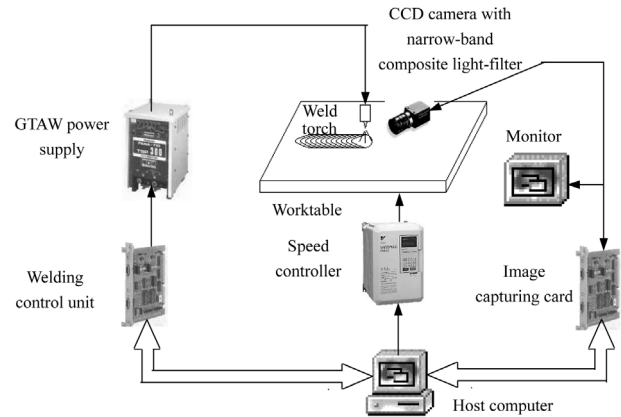
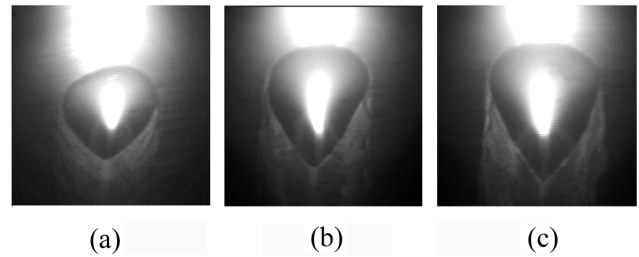


**Figure 2** The raw images of weld pool: (a) 100, (b) 105 and (c) 110 A



An image-processing algorithm is developed for determining the pool geometry, which includes the following steps.

### 2.1 Preprocessing

There are quite a few steps for capturing weld pool images, that is, sampling, digitising, transmitting and so on. During this process, the digitised images (grey value matrixes) contain some noises because of disturbances. On the other hand, they also have problems of low contrast and obscure edges. To remove the disturbances and improve the image quality, preprocessing of the digitised images has to be conducted before extracting information about the weld pool edges. To this end, the preprocessing is carried out on the basis of the following equations.

Along the  $x$ -direction (perpendicular to the weld line, that is, longitudinal section in Figure 2):

Firstly, a digital filter is designed to eliminate noises, that is,

$$q(i+1, j) = \frac{g_0(i+2, j) + 2g_0(i+1, j) + g_0(i, j)}{4} \quad (1a)$$

$$q(i, j) = \frac{g_0(i+1, j) + 2g_0(i, j) + g_0(i-1, j)}{4} \quad (1b)$$

Then, a differential operator is applied to sharpen the weld pool boundary (image-enhancement) as follows:

$$g(i, j) = k_1 + k_2[q(i+1, j) - q(i, j)] \quad (1c)$$

To combine the noise-elimination (1a and 1b) with the image-enhancement (1c) together, we obtain:

$$g(i, j) = k_1 + k_2 \frac{g_0(i+2, j) + g_0(i+1, j) - g_0(i, j) - g_0(i-1, j)}{4} \quad (1d)$$

Similarly, we obtain the algorithm along the  $y$ -direction (weld line direction, i.e. vertical direction in Figure 2):

$$g(i, j) = k_1 + k_2 \frac{g_0(i, j+2) + g_0(i, j+1) - g_0(i, j) - g_0(i, j-1)}{4} \quad (2)$$

where  $g(i, j)$  and  $g_0(i, j)$  are the grey values of point  $(i, j)$  in the matrix after and before processing, respectively.  $k_1$  and  $k_2$  are the adjustment coefficient and enhancement coefficient, respectively.

## 2.2 Extracting the edges of weld pool

After preprocessing, the distribution of grey values  $g(i, j)$  in the digitised image has the following characteristic: along the  $x$ -direction, the weld pool boundary locates between the valley and peak of grey levels for left and right edges, respectively. For convenience, the whole weld pool boundary is divided into three sections: right, left and rear edges. The heuristic edge tracking is used to search the weld pool edges. The key is to design a good evaluation function. The evaluation functions are designed as follows.

For the right edges:

$$\rho_{\text{right}}(i, j) = \varphi_1 \varphi_2 \mu(d) \quad (3)$$

where

$$\varphi_1 = \begin{cases} 1 & \text{for } g(i, j) = \max[g(i-2, j), \\ & g(i-1, j), \dots, g(i+1, j), g(i+2, j)] \\ 0 & \text{for other case} \end{cases}$$

$$\varphi_2 = g(i, j)$$

$\mu(d)$  is the membership function to the edges (the value of  $\mu(d)$  is between 0 and 1),  $d$  is the distance between the dot  $(i, j)$  and the nearest right edge point. For the right edges,  $\varphi_2 = g(i, j)$  has the maximum value (peak) based on Equation (1d). Thus, to make the point with the maximum of  $\rho_{\text{right}}$  as the edge point, the value of  $\rho_{\text{right}}$  is taken as the product of  $\varphi_1$  and  $\varphi_2$  multiplied by  $\mu(d)$ .

For the left edges:

$$\rho_{\text{left}}(i, j) = \frac{\varphi_1 \varphi_2}{\mu(d)} \quad (4)$$

where

$$\varphi_1 = \begin{cases} 1 & \text{for } g(i, j) = \min[g(i-2, j), \\ & g(i-1, j), \dots, g(i+1, j), g(i+2, j)] \\ 0 & \text{for other case} \end{cases}$$

$$\varphi_2 = g(i, j)$$

$\mu(d)$  has the same meaning as in Equation (3),  $d$  is the distance between the dot  $(i, j)$  and the nearest left edge point. For the left edges,  $\varphi_2 = g(i, j)$  has the minimum value (valley) based on Equation (1d). Thus, to make the point with the minimum of  $\rho_{\text{left}}$  except 0 as the edge point, the value of  $\rho_{\text{right}}$  is taken as the product of  $\varphi_1$  and  $\varphi_2$  divided by  $\mu(d)$ .

For the rear edges:

$$\rho_{\text{rear}}(i, j) = \varphi_1 \varphi_2 \mu(d) \quad (5)$$

where

$$\varphi_1 = \begin{cases} 1 & \text{for } g(i, j) = \max[g(i, j-2), \\ & g(i, j-1), \dots, g(i, j+1), g(i, j+2)] \\ 0 & \text{for other case} \end{cases}$$

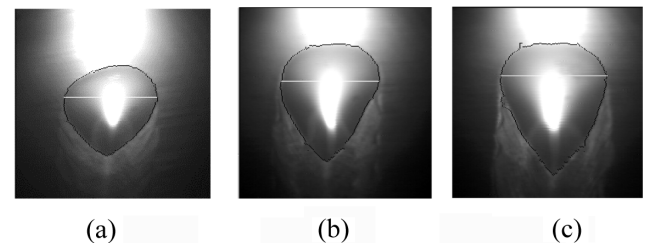
$$\varphi_2 = g(i, j)$$

$\mu(d)$  has the same meaning and value as in Equation (3),  $d$  is the distance between the dot  $(i, j)$  and the nearest rear edge point. The point with the maximum of  $\rho_{\text{rear}}$  is taken as the edge point.

For searching the weld pool edges, firstly, find a line that has a marked characteristic of edge points, recorded as line  $j_0$ . Secondly, preprocessing and heuristic edge tracking along  $x$ -direction is carried out from the line  $j_0$  towards to the upper part of images until  $\rho_{\text{right}} = 0$  or  $\rho_{\text{left}} = 0$  for all points twice. Thirdly, preprocessing and heuristic edge tracking along  $x$ -direction is made from the line  $j_0$  towards to the lower part of the image until  $\rho_{\text{right}} = 0$  or  $\rho_{\text{left}} = 0$  for all points twice and this line is recorded as line  $j_{\text{end}}$ . The  $x$  coordinate of the left edge point and right edge point of this line is recorded by  $\text{edge}_l[j_{\text{end}}]$  and  $\text{edge}_r[j_{\text{end}}]$ , respectively. Finally, starting from  $\text{edge}_l[j_{\text{end}}]$  vertical line, preprocessing and heuristic edge tracking along  $y$ -direction is done to find the edge point of the rear part of the weld pool image until the vertical line  $\text{edge}_r[j_{\text{end}}]$  is encountered.

Figures 2 and 3 show the original images and processed images of weld pool at different levels of welding current.

**Figure 3** The processed images of weld pool: (a) 100, (b) 105 and (c) 110 A



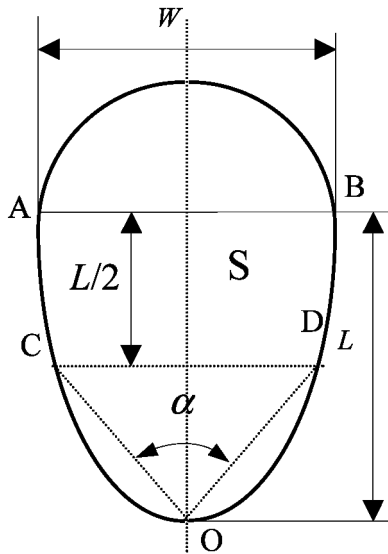
## 2.3 Determining the geometrical parameters of weld pool

After extracting the edge points of weld pool images, the coordinates of left edge points, the right edge points and the rear edge points are obtained. According to the position of the rear edge points, it can be divided into left edge points and right edge points. Thus, the weld pool geometry

can be expressed by the left edge points and the right edge points. Coordinates of the left edge point and the right edge point in line  $j$  are stored in vector variables  $edge_l[j]$  and  $edge_r[j]$ , respectively.

As the actual size of weld pool is different from the size of digital image, the calibration must be carried out. In the system, a pixel represents 0.1071 and 0.2612 mm, along  $x$ - and  $y$ -direction, respectively. To describe the weld pool geometry, four geometrical parameters of weld pool are defined, that is, the maximum width  $W$ , half length  $L$ , rear angle  $\alpha$  and rear area  $S$ . Figure 4 demonstrates the definition of the geometrical parameters of a weld pool. The rear area  $S$  is the area surrounded by the solid curve ACODB.

**Figure 4** The definition of surface geometrical parameters of weld pool



### 3 Modelling and controller design

Weld pool images provide abundant weld penetration information (Kovacevic et al., 1996). If the surface geometry of weld pool is known, a neural network can be developed to correlate the surface geometry of weld pool with the BW, so that the degree of penetration can be predicted. Thus, the main task here is to set up a neural network for predicting the BW through using the pool surface geometry parameters such as the rear length of weld pool ( $L$ ), the maximum width of weld pool ( $W$ ), the rear angle of weld pool ( $\alpha$ ) and the rear area of weld pool ( $S$ ). Such a model is referred to as the FBW model.

#### 3.1 FBW model

To obtain enough experimental data, ten sets of experiments are conducted, which demonstrate the change of three main welding parameters, such as welding current, welding speed and arc length. Experiments are conducted on mild steel Q235 with a size of 200 mm  $\times$  50 mm  $\times$  3 mm and bead-on-plate welding is also conducted. The sampling frequency of image capturing is 1 Hz. A total of 1052 groups of data are

obtained, which covers the full penetration conditions on the workpiece, and one group of geometrical parameters of the weld pool corresponds to one image.

As welding process is characterised by thermal accumulation and thermal lag, only the present values of the surface geometrical parameters of weld pool cannot precisely reflect the BW. Therefore, the historic values of these parameters must be considered in the model. As shown in Figure 5, a three-layer neural network is developed to determine the relationship between the present values and historic values of surface geometrical parameters of weld pool and the BW. The model takes the present values and the previous values of  $W$ ,  $L$ ,  $S$ ,  $\alpha$  as input parameters and the BW as the output parameter. Figure 6 shows the comparison of the FBW model output to the experimental results.

**Figure 5** The structure of FBW model

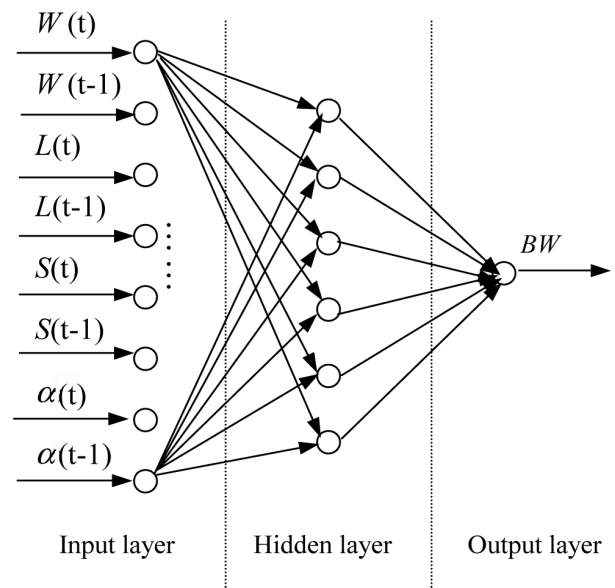
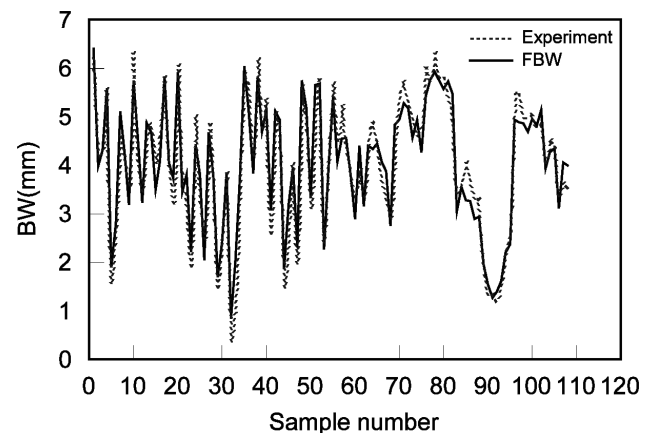


**Figure 6** Testing the validity of the FBW model

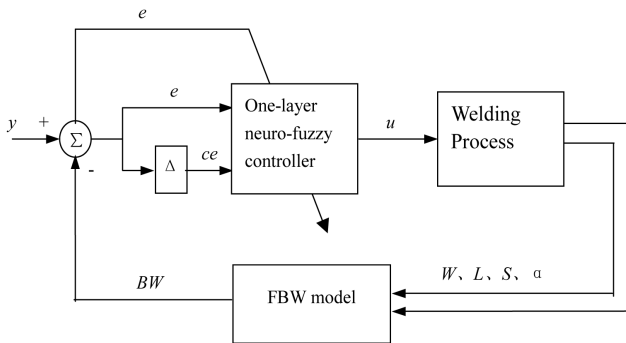


#### 3.2 Fuzzy rules and inference

The welding current is selected as the control variable and the BW is selected as the controlled variable. The input of the fuzzy controller includes the error and the error variation as shown in Figure 7 while the output variable is the change of welding current. The error is the difference

between the desired value and actual value of the BW. The error variation is the difference between the error at present sampling moment and the error at last sampling moment. Here, the symbols  $e$  and  $ce$  denote the exact values of error and the error variation, respectively.  $E$  and  $CE$  are the corresponding fuzzy variables.  $E$  and  $CE$  are all divided into seven fuzzy subsets and seven linguistic terms are used to express those subsets. They are Negative Big (NB), Negative Medium (NM), Negative Small (NS), Zero (O), Positive Small (PS), Positive Medium (PM) and Positive Big (PB). The membership functions of linguistic terms are in the form of isosceles triangle.

**Figure 7** Self-learning block diagram of one-layer neuro-fuzzy controller



A special form of Takagi-Sugeno fuzzy rules is adopted (Jing, 1998). That is, the premise variable is still expressed by linguistic terms while the result variable is expressed by an exact value. The fuzzy rules take, for example, the following form:

If  $E$  is NB and  $CE$  is NB, then  $w$  is  $w_1$  (the certainty factor is  $a'_1$ , which will be given later).

All fuzzy rules are tabulated in Table 1. The values of  $w_1, w_2, \dots, w_{49}$  in the fuzzy rules are obtained automatically by the one-layer neuro-fuzzy network (Figure 7) online or offline and can be revised according to the variation of test conditions automatically.

**Table 1** The fuzzy rules of neuro-fuzzy controller

	NB	NM	NS	O	PS	PM	PB
NB	$w_1$	$w_2$	$w_3$	$w_4$	$w_5$	$w_6$	$w_7$
NM	$w_8$	$w_9$	$w_{10}$	$w_{11}$	$w_{12}$	$w_{13}$	$w_{14}$
NS	$w_{15}$	$w_{16}$	$w_{17}$	$w_{18}$	$w_{19}$	$w_{20}$	$w_{21}$
O	$w_{22}$	$w_{23}$	$w_{24}$	$w_{25}$	$w_{26}$	$w_{27}$	$w_{28}$
PS	$w_{29}$	$w_{30}$	$w_{31}$	$w_{32}$	$w_{33}$	$w_{34}$	$w_{35}$
PM	$w_{36}$	$w_{37}$	$w_{38}$	$w_{39}$	$w_{40}$	$w_{41}$	$w_{42}$
PB	$w_{43}$	$w_{44}$	$w_{45}$	$w_{46}$	$w_{47}$	$w_{48}$	$w_{49}$

Assuming that the exact value of error and the error variation is  $e_i$  and  $ce_i$  after scaled by  $k_e$  and  $k_{ce}$ , the change of welding current can be calculated as follows.

The certainty factor of the  $k$ th rule is

$$a'_k = \frac{a_k}{\sum_{m=1}^{49} a_m} \tag{6}$$

where

$$a_k = \min[\mu_{E_{k1}}(e_i), \mu_{CE_{k2}}(ce_i)] \tag{7}$$

where  $E_{k1}$  and  $CE_{k2}$  are the fuzzy subset of error and error variation corresponding to the  $k$ th rule, respectively.  $\mu$  is the membership function.

The output of the fuzzy controller is, thus:

$$o = \sum_{m=1}^{49} a'_m w_m \tag{8}$$

### 3.3 Neural network realising fuzzy inference and its learning algorithm

The above fuzzy inference may be realised by the one-layer neuro-fuzzy network (Figure 7). The number of input nodes of neural network is 49. Each node is corresponding to a fuzzy rule. The input of each node is the certainty factor of the corresponding fuzzy rule. There is only one output node. It is the change of control variable, that is, the welding current.

The gradient of Sigmoid function (S function) is steeper at middle part and flatter at two ends. This characteristic is similar to that of biological neural cells. Also the S function has characteristics of non-linearity and differentiability, thus enhancing the non-linear map ability of neural network. Therefore, the S function is employed as the nodes output transfer function of neural nodes. The S function is as follows:

$$u' = \frac{1}{1 + \exp(-o + \theta)} \tag{9}$$

$$o = \sum_{m=1}^{49} a'_m w_m \tag{10}$$

where  $\theta$  is the node threshold.

As the output [0, 1] of S function is not in the range of the output variable, the linear transformation should be done as follows:

$$u = u'(u_{\max} - u_{\min}) + u_{\min} \tag{11}$$

where  $u_{\max}$  is the maximum value of the output variable and is ended with 15 A, while  $u_{\min}$  is the minimum value -15 A.

As the ideal output of the control variable is unknown in welding process, the conventional back propagation algorithm is used to guarantee that the learning algorithm of the neural network of controller can proceed smoothly. According to the algorithm, the variation of connection weight of neural network is

$$\Delta w_m(k) = -\eta \frac{\partial G(k)}{\partial w_m(k)} \tag{12}$$

where  $w_m(k)$  is the connection weight of the neural network,  $\eta$  is the learning rate,  $G(k)$  is the output error of the neural network,  $G(k) = 1/2 (u_{id} - u)^2$ ,  $u_{id}$  and  $u$  are the  $k$ th desired and actual output errors of the neural network, respectively.

As  $u_{id}$  is unknown in system design, the output error of object controlled  $G(k) = 1/2 (bw_{id} - bw)^2$  is used instead of that of the neural network ( $bw_{id}$  and  $bw$  are the  $k$ th desired and actual output errors of the BW, respectively), thus the following equation can be obtained:

$$\frac{\partial G(k)}{\partial w_m(k)} = \frac{\partial G(k)}{\partial bw(k)} \frac{\partial bw(k)}{\partial u(k)} \frac{\partial u(k)}{\partial u'(k)} \frac{\partial u'(k)}{\partial w_m(k)} \quad (13)$$

where  $\partial bw(k)/\partial u(k)$  is approximately substituted by  $\Delta bw(k)/\Delta u(k)$ , thus Equation (12) can be written as follows:

$$\Delta w_m(k) = \eta [bw_{id}(k) - bw(k)] \frac{\Delta bw(k)}{\Delta u(k)} (u_{max} - u_{min}) u'(1 - u') a'_m \quad (14)$$

where  $bw_{id}(k)$  is the desired output of the BW.

Equation (14) can be written as follows:

$$\Delta w_m(k) = \eta \delta(k) a'_m \quad (15)$$

where

$$\delta(k) = [bw_{id}(k) - bw(k)] \frac{\Delta bw(k)}{\Delta u(k)} (u_{max} - u_{min}) u'(1 - u')$$

The variation of threshold is as follows:

$$\Delta \theta(k) = \beta \delta(k) \quad (16)$$

where  $\beta$  is the learning rate.

At the beginning, the initial values of  $w_m$  and  $\theta$  may be selected arbitrarily. Then, they are improved step by step as follows:

$$w_m(k+1) = w_m(k) + \Delta w_m(k) \quad (17)$$

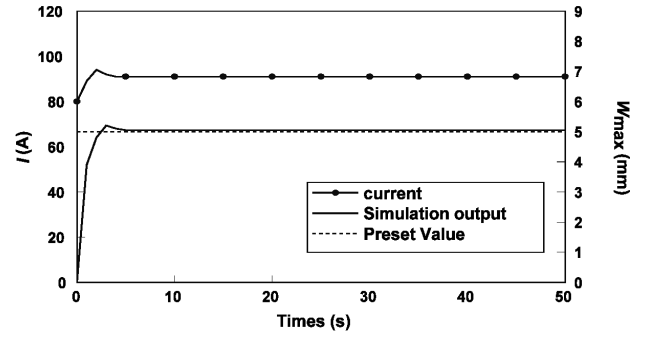
$$\theta(k+1) = \theta(k) + \Delta \theta(k) \quad (18)$$

By employing the learning algorithm mentioned above, the values of  $w_m (m = 1, 2, \dots, 49)$  in the fuzzy rules can be determined automatically from the one-layer neuro-fuzzy network (Figure 7). Therefore, the output of the control variable  $u$  (the change of welding current) is obtained from Equations (9)–(11).

#### 4 Simulation and controls experiment

In this study, the control target of the BW is 5 mm. Figure 8 shows the simulation result of the controller. It shows that the overshoot of the BW is 4.0%, and the regulating time is 4 sec. The static error of the BW is 0.05 mm. The welding current stabilises at 91 A. The simulation results show that the controller has good control performance.

**Figure 8** The simulation result of the controller



To examine the validity of the control system, the workpiece with a neck showed in Figure 9 is used, which reflects the variation of thermal conduction when the cross-section of the workpiece is suddenly changed. The material of workpiece is mild steel Q235. The welding speed is 69 mm/min, the arc length is 5.2 mm, the shielding gas (Ar) flow rate is 15 l/min. The curve of BW in open-loop condition is shown in Figure 10. It can be seen that the BW increases when the cross-section of workpiece changes from wider to narrower and decreases when the cross-section changes from narrower to wider. This is because the heat transfer condition changes with the variation of cross-section. The range of BW is  $\sim 4.12$ – $8.88$  mm. The control result of the neuro-fuzzy controller is shown in Figure 11. It can be seen that the welding current is apparently lower in the middle part of the workpiece while it is higher in the other part of the workpiece. The welding current in the end part of workpiece is lower than the start part of the workpiece because of heat accumulation. The value of BW is  $\sim 4.76$ – $5.55$  mm. Thus, the control result is satisfactory.

**Figure 9** Sketch of the shape of workpiece with varied section

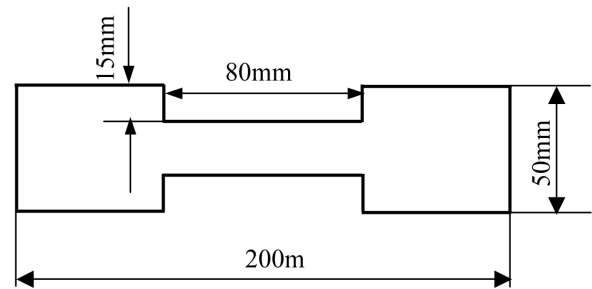


**Figure 10** The BW of varied section workpiece in open-loop condition

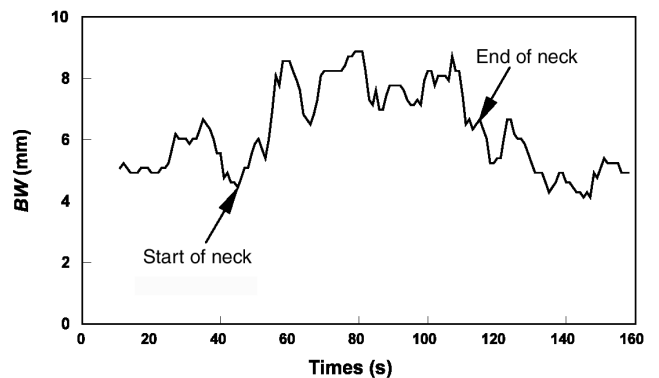
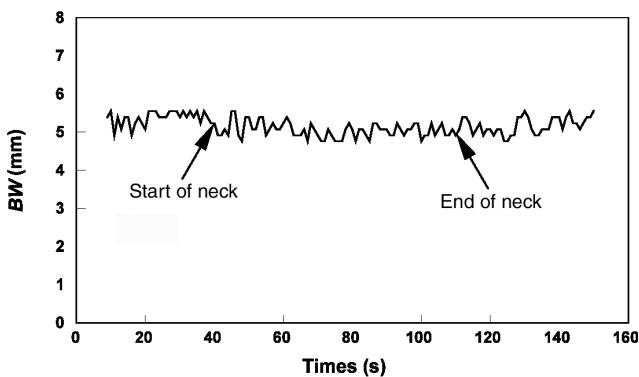
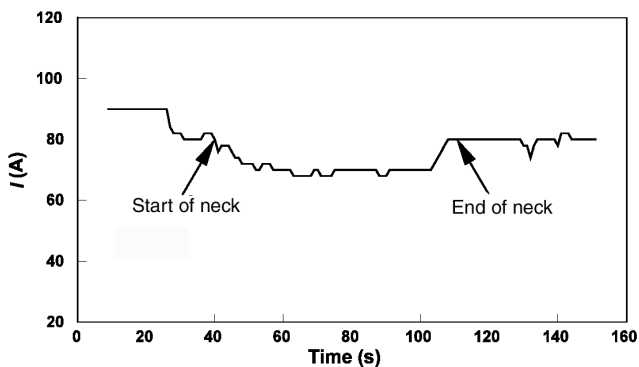


**Figure 11** The control result of neuro-fuzzy controller: (a) BW variation and (b) welding current variation



(a)



(b)

## 5 Conclusions

- 1 A vision sensor consisting of a CCD camera and a special narrow-band pass filter can capture images of the weld pool during the GTAW process. By employing the developed image processing software, the geometrical parameters of the weld pool, such as the maximum width  $W$ , half length  $L$ , rear area  $S$  and rear angle  $\alpha$ , can be determined.
- 2 A model FBW describing the relationship between the weld pool geometrical parameters and the BW is constructed. The model inputs are the present values and the previous values of  $W$ ,  $L$ ,  $S$ ,  $\alpha$ .

- 3 A neuro-fuzzy controller is developed considering non-linearity, time-dependence and long time delay of the welding process. The input variables of the controller are the error and the error variation of the BW and the output variable is the change of welding current.
- 4 As the ideal output of the control variable is unknown in welding process, the conventional back propagation algorithm is advised to guarantee that the learning algorithm of the neural network of controller can be proceeded smoothly.
- 5 The simulation and experimental results show that the system has good control performance and satisfactory control accuracy.

## Acknowledgement

This work is supported by the Natural Science Foundation of Shandong Province in China (Grant No. Z2003F05).

## References

- Gao, J.Q. and Wu, C.S. (2001) 'Experimental determination of weld pool geometry in gas tungsten arc welding', *Science and Technology of Welding and Joining*, Vol. 6, No. 5, pp.1–5.
- Huang, S.S., He, J.F. and Song, Y.L. (1996) 'Design of fuzzy logic controller for bead width of GTAW', *Transactions of the China Welding Institution*, Vol. 17, No. 2, pp.159–164.
- Jing, Y.W. (1998) 'Design of robust controller for dynamic time-delay system via viewer', *Control and Decision*, Vol. 13, No. 5, pp.581–588.
- Kovacevic, R. and Zhang, Y.M. (1995) 'Machine vision recognition of weld pool in gas tungsten arc welding', *Proceedings of the Institutions of Mechanical Engineers, Part B: Journal of Engineering Manufacture*, Vol. 209, pp.141–152.
- Kovacevic, R., Zhang, Y.M. and Li, L. (1996) 'Monitoring of weld joint penetration based on weld pool geometrical appearance', *Welding Journal*, Vol. 75, pp.317s–329s.
- Pietrzak, K.A. and Packer, S.M. (1994) 'Vision-based weld pool width control', *ASME Transaction, Journal of Engineering for Industry*, Vol. 116, pp.86–92.
- Zhang, Z.D. (1997) 'Artificial neural network estimating spot welding mechanical property', *Transactions of the China Welding Institution*, Vol. 18, No. 1, pp.1–5.